Spatial and temporal regulation of cofilin activity by LIM kinase and Slingshot is critical for directional cell migration

Michiru Nishita, Chinatsu Tomizawa, Masahiro Yamamoto, Yuji Horita, Kazumasa Ohashi, and Kensaku Mizuno

Department of Biomolecular Sciences, Graduate School of Life Sciences, Tohoku University, Sendai, Miyagi 980-8578, Japan

Cofilin mediates lamellipodium extension and polarized cell migration by accelerating actin filament dynamics at the leading edge of migrating cells. Cofilin is inactivated by LIM kinase (LIMK)–1-mediated phosphorylation and is reactivated by cofilin phosphatase Slingshot (SSH)-1L. In this study, we show that cofilin activity is temporally and spatially regulated by LIMK1 and SSH1L in chemokine-stimulated Jurkat T cells. The knockdown of LIMK1 suppressed chemokine-induced lamellipodium formation and cell migration, whereas SSH1L knockdown produced and retained multiple lamellipodial protrusions around the cell after cell stimulation and impaired directional cell migration. Our results indicate that LIMK1 is required for cell migration by stimulating lamellipodium formation in the initial stages of cell response and that SSH1L is crucially involved in directional cell migration by restricting the membrane protrusion to one direction and locally stimulating cofilin activity in the lamellipodium in the front of the migrating cell. We propose that LIMK1- and SSH1L-mediated spatiotemporal regulation of cofilin activity is critical for chemokine-induced polarized lamellipodium formation and directional cell movement.

Introduction

Chemotaxis plays an essential role in both physiological and pathological events, including embryogenesis, immune responses, wound healing, and tumor metastasis (Franz et al., 2002). When exposed to chemotactic factors, cells become polarized and form an F-actin–rich lamellipodial membrane protrusion toward the direction of cell movement; this protrusion is maintained at the leading edge during migration (Pollard and Borisy, 2003; Ridley et al., 2003). In the lamellipodium, there are polarized and dendritic arrays of actin filaments with fast growing "barbed" ends near the plasma membrane and slow growing "pointed" ends at the rear (Welch et al., 1997; Pollard and Borisy, 2003). Actin polymerization near the plasma membrane forces the membrane to move forward, whereas the rear is continuously disassembled to replenish actin monomers for further polymerization at the leading edge of the cell (Cramer, 1999; Pollard and Borisy, 2003).

Cofilin is a potent regulator of actin filament dynamics and mediates the rapid turnover of actin filaments by severing actin filaments and by stimulating actin filament disassembly near the pointed ends (Moon and Drubin, 1995; Theriot, 1997; Bamburg, 1999; Pantaloni et al., 2001; Bamburg and Wiggan, 2002; Hotulainen et al., 2005). Cofilin appears to play a key role in maintaining and extending the lamellipodial protrusion at the leading edge of migrating cells (Bailly and Jones, 2003; Dawe et al., 2003). Cofilin is inactivated by LIM kinase (LIMK) or related testicular kinase (TESK) through the phosphorylation of Ser-3 (Arber et al., 1998; Yang et al., 1998; Toshima et al., 2001). This phosphorylation inhibits the interactions of cofilin with actin filaments and actin monomers. The overexpression of LIMK1, which inactivates cellular cofilin, impairs the formation of polarized cell morphology and directional cell migration, which suggests that cofilin plays a crucial role in cell polarity formation and directional cell migration (Dawe et al., 2003). Notably, although LIMK1 inhibits cofilin, it is activated in Jurkat T cells in response to stromal cell–derived factor-1α (SDF-1α), which is a member of the Cys-X-Cys–type chemokine family, and the inhibition of LIMK1 activity by a cell-permeable cofilin-derived peptide blocks SDF-1α–induced chemotaxis of Jurkat cells (Nishita et al., 2002). These observations suggest that LIMK1 is required for chemotaxis, but the mechanism involved remains unclear.

M. Nishita, C. Tomizawa, and M. Yamamoto contributed equally to this paper.

Correspondence to Kensaku Mizuno: kmizuno@biology.tohoku.ac.jp

Abbreviations used in this paper: LIMK, LIM kinase; P-cofilin, Ser-3–phosphorylated cofilin; PI3K, phosphatidylinositol-3 kinase; SDF-1α, stromal cell–derived factor-1α; siRNA, small interfering RNA; sr, siRNA resistant; SSH, Slingshot; WT, wild type.

The online version of this article contains supplemental material.

The Journal of Cell Biology, Vol. 171, No. 2, October 24, 2005 349–359
http://www.jcb.org/cgi/doi/10.1083/jcb.200504029

The inactive Ser-3–phosphorylated cofilin (P-cofilin) is dephosphorylated and reactivated by Slingshot (SSH) family cofilin phosphatases, including SSH1L, -2L, and -3L (Niwa et al., 2002; Ohta et al., 2003) or chronophin, which is a member of haloacid dehalogenases (Gohla et al., 2005). We have shown that SSH1L is highly activated by its association with F-actin in cell-free assays and that it accumulates in the F-actin–rich lamellipodium after stimulation of carcinoma cells with neuregulin or insulin (Nagata-Ohashi et al., 2004; Nishita et al., 2004). This suggests that SSH1L is locally activated in the lamellipodium in response to cell stimulation and may be involved in the spatial regulation of cofilin activity. However, it remains unclear whether F-actin–mediated SSH1L activation is required for directional cell migration.

In this study, we investigated the role cofilin phosphoregulation plays in the chemotactic migration of Jurkat cells in response to SDF-1α. We show that cofilin activity is temporally and spatially regulated by LIMK1 and SSH1L in Jurkat T cells that are stimulated with SDF-1α. Knocking down LIMK1, SSH1L, or cofilin expression by small interfering RNA (siRNA) suppresses chemokine-induced polarized F-actin assembly and chemotactic responses of Jurkat cells. We provide evidence that LIMK1 is required for cell migration by stimulating lamellipodium formation in the early stages of cell response. Furthermore, SSH1L is critically involved in directional cell migration by restricting the membrane protrusion to one direction in the early stages of cell response and then locally stimulating cofilin activity in the lamellipodium at the leading edge of the migrating cell. In addition, we identified Trp-458 as a critical residue for SSH1L to be activated by F-actin. By using an F-actin–insensitive SSH1L mutant in which Trp-458 is mutated, we show that F-actin–mediated SSH1L activation is required for the chemotactic response of Jurkat cells. Therefore, we propose that LIMK1- and SSH1L-mediated spatiotemporal regulation of cofilin activity plays a critical role in chemokine-induced polarized cell migration.

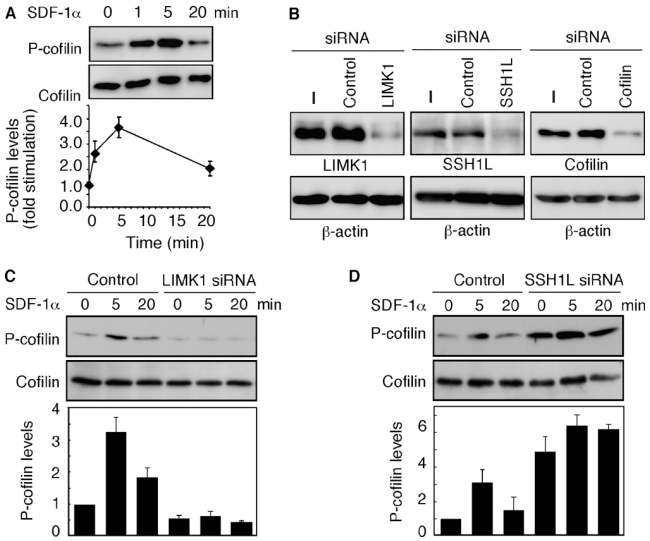

Figure 1. **SDF-1α–induced changes in P-cofilin levels are regulated by LIMK1 and SSH1L.** (A) SDF-1α–induced changes in P-cofilin levels. Jurkat cells were stimulated with 5 nM SDF-1α for the indicated times, and cell lysates were analyzed by immunoblotting with anti–P-cofilin and anticofilin antibodies. The bottom panel shows the relative P-cofilin levels after SDF-1α stimulation as means ± SEM of triplicate experiments. (B) Suppression of endogenous LIMK1, SSH1L, and cofilin expression by siRNA. Jurkat cells were transfected with siRNA plasmids for GFP (control), LIMK1, SSH1L, cofilin, or empty vector (−). After 60 h of culture, cell lysates were analyzed by immunoblotting with antibodies specific for each protein and β-actin. For LIMK1 and SSH1L, the cell lysates were subjected to immunoblotting after immunoprecipitation. (C and D) Effects of LIMK1 or SSH1L siRNA on SDF-1α–induced changes in P-cofilin levels. SSH1L, LIMK1, or GFP (control) siRNA cells were stimulated with 5 nM SDF-1α. Cell lysates, prepared at the indicated times, were analyzed by immunoblotting as in A. The bottom panels indicate the relative P-cofilin levels; the value at time = 0 in control cells is taken as 1.0. Each value represents the mean ± SEM (error bars) of triplicate experiments.

Results

Cofilin activity is temporally regulated by LIMK1 and SSH1L in SDF-1α–stimulated Jurkat cells

Cofilin activity is negatively regulated by phosphorylation at Ser-3. To examine the role cofilin phosphoregulation plays in T cell chemotaxis, we first analyzed time-dependent changes in P-cofilin levels in Jurkat cells after SDF-1α stimulation. The P-cofilin levels increased by 1–5 min as reported previously (Nishita et al., 2002) but reverted to basal levels 20 min after SDF-1α stimulation (Fig. 1 A). Because LIMK1 in Jurkat cells is activated by SDF-1α for up to 20 min (Nishita et al., 2002), the decrease in P-cofilin levels at 20 min probably involves the activation of cofilin phosphatases such as SSH1L. To assess the roles of LIMK1 and SSH1L in the SDF-1α–induced changes in P-cofilin levels, we knocked down LIMK1 and SSH1L expression using siRNA. Endogenous LIMK1 and SSH1L expression was suppressed by the transfection of siRNA plasmids (Fig. 1 B). LIMK1 siRNA reduced the basal P-cofilin levels in unstimulated cells and inhibited the increase in P-cofilin levels that occurred 5 min after SDF-1α stimulation (Fig. 1 C). In contrast, SSH1L siRNA raised the basal P-cofilin levels, and these levels were further augmented at 5 and 20 min after SDF-1α stimulation (Fig. 1 D). These results suggest that LIMK1 plays a critical role in the SDF-1α–induced elevation of P-cofilin levels at 5 min and that SSH1L is involved in decreasing P-cofilin levels in later stages after SDF-1α stimulation.

Subcellular localization of LIMK1, SSH1L, and cofilin in SDF-1α–stimulated Jurkat cells

When exposed to SDF-1α, Jurkat cells produced multiple membrane protrusions around the cell at 1 min and became polarized to form a single lamellipodial protrusion in one direction by 5 min (Fig. 2, A and B; and Video 4, available at http://www.jcb.org/cgi/content/full/jcb.200504029/DC1). We examined the temporal changes in the distribution of LIMK1 and SSH1L before and after SDF-1α stimulation by coexpressing CFP-LIMK1 and YFP-SSH1L in Jurkat cells. Fluorescence microscopic analyses after fixing the cells showed that CFP-LIMK1 was diffusely distributed in the cytoplasm both before and after SDF-1α stimulation, whereas YFP-SSH1L was diffusely distributed in the cytoplasm in unstimulated cells but

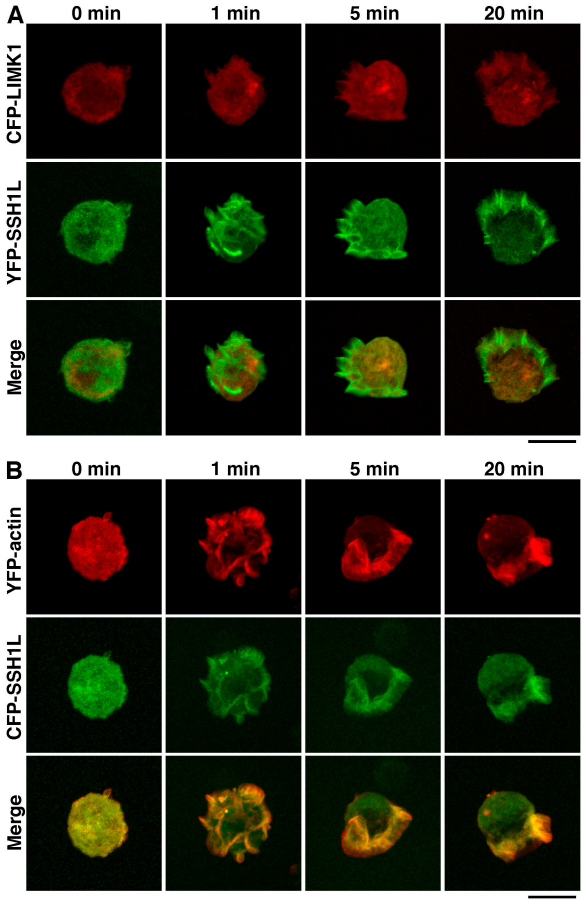

Figure 2. **Temporal localization of LIMK1 and SSH1L in SDF-1α–stimulated Jurkat cells.** (A) Localization of CFP-LIMK1 (red) and YFP-SSH1L (green) in fixed Jurkat cells unstimulated (0 min) or stimulated for 1, 5, and 20 min with 5 nM SDF-1α. Merged images are shown in the bottom panels. (B) Localization of YFP-actin (red) and CFP-SSH1L (green) in fixed Jurkat cells unstimulated (0 min) or stimulated for 1, 5, and 20 min with 5 nM SDF-1α. Merged images are shown in the bottom panels. Bars, 5 μm.

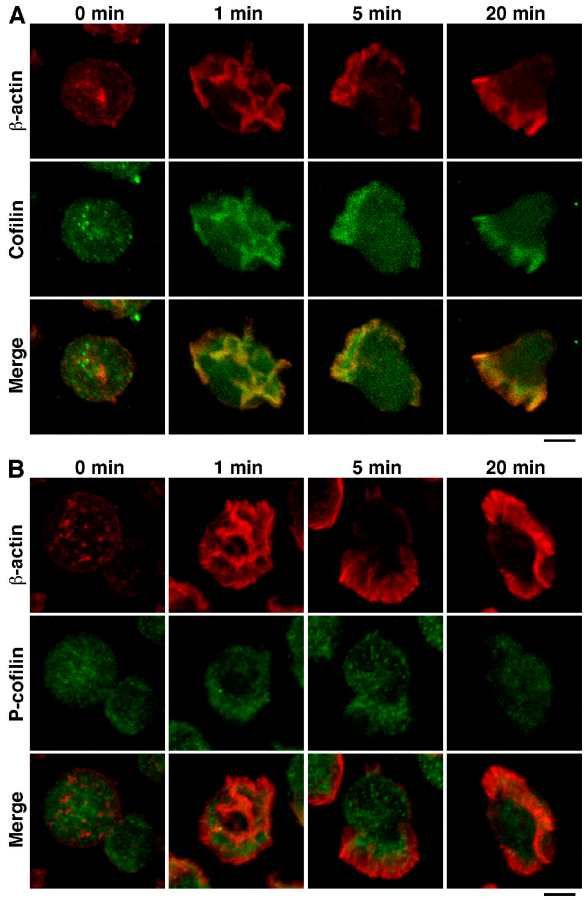

Figure 3. **Cofilin, but not P-cofilin, accumulates in the SDF-1α–induced lamellipodial membrane protrusion in Jurkat cells.** Jurkat cells were left unstimulated (0 min) or were stimulated with 5 nM SDF-1α for the indicated periods of time. Cells were costained with anti–β-actin mAb (red) and anti-cofilin (A) or anti–P-cofilin (B) pAbs (green). Merged images are shown in the bottom panels. Bars, 5 μm.

accumulated in the lamellipodial protrusions 1–20 min after SDF-1α stimulation (Fig. 2 A). The three-dimensional projection image more clearly showed the distinct distribution of LIMK1 and SSH1L in Jurkat cells that were stimulated for 5 min (Video 1, available at http://www.jcb.org/cgi/content/full/jcb.200504029/DC1). Time-lapse live-cell image analyses of CFP-LIMK1 and YFP-SSH1L also showed that LIMK1 was diffusely distributed and that SSH1L accumulated in membrane protrusions after SDF-1α stimulation (Video 2). We also analyzed the temporal localization of YFP-actin and CFP-SSH1L in fixed (Fig. 2 B) and live Jurkat cells (Video 3). Both analyses revealed that CFP-SSH1L was diffusely distributed in the cytoplasm before SDF-1α stimulation, but it almost colocalized with YFP-actin and accumulated in the F-actin–rich lamellipodia after stimulation. It appears from the merged images that SSH1L is depleted from the tip of the lamellipodium (Fig. 2 B).

We next examined the temporal distribution of cofilin and P-cofilin in Jurkat cells before and after SDF-1α stimulation (Fig. 3). Cell staining with cofilin- or P-cofilin–specific antibodies and β-actin antibody revealed that cofilin, but not P-cofilin, accumulated in F-actin–rich membrane protrusions after SDF-1α stimulation. In unstimulated cells, both cofilin and P-cofilin diffusely distributed in the cytoplasm. These data indicate that the active (unphosphorylated) form of cofilin is preferentially concentrated in the lamellipodium after SDF-1α stimulation. Localization of cofilin, but not P-cofilin, in the lamellipodium was also noted in migrating fibroblasts and carcinoma cells (Dawe et al., 2003; Nagata-Ohashi et al., 2004). Because SSH1L is activated by associating with F-actin, these findings suggest that the SSH1L molecules recruited to the F-actin–rich lamellipodium are activated and may be involved in local dephosphorylation/activation of cofilin in this region.

Effects of LIMK1, SSH1L, or cofilin knockdown on T cell chemotaxis and chemokinesis

To examine the roles that SSH1L, LIMK1, and cofilin play in SDF-1α–induced T cell migration, the expression of each protein in Jurkat cells was suppressed by siRNA (Fig. 1 B), and the directional (chemotactic) and random (chemokinetic) migration of these cells in response to SDF-1α was analyzed by using Transwell culture chambers (Fig. 4). SDF-1α was added only to the lower chamber to analyze the chemotactic response,

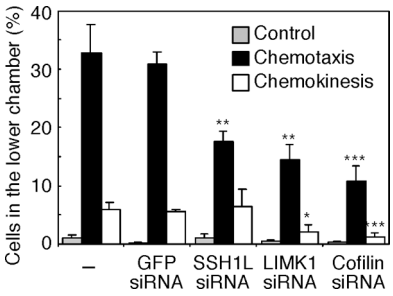

Figure 4. **Effect of SSH1L, LIMK1, or cofilin siRNA on SDF-1α–induced T cell chemotaxis and chemokinesis.** Jurkat cells were transfected with siRNA plasmids for GFP (control), SSH1L, LIMK1, cofilin, or empty vector (−) as indicated. Chemotactic responses toward 5 nM SDF-1α and chemokinetic responses in the presence of 5 nM SDF-1α were determined in the Transwell culture chambers, as described in Materials and methods. The data are expressed as the means ± SEM (error bars) of three independent experiments. *, $P < 0.05$; **, $P < 0.01$; ***, $P < 0.005$, compared with cells transfected with the empty vector.

whereas it was added to both the lower and upper chambers for chemokinesis assays. The knockdown of either SSH1L, LIMK1, or cofilin by siRNA significantly reduced the chemotactic response of Jurkat cells toward SDF-1α (Fig. 4), which indicates that SSH1L, LIMK1, and cofilin all play critical roles in T cell chemotaxis. In contrast, the chemokinetic response of cells was suppressed by LIMK1 or cofilin siRNA but not by SSH1L siRNA (Fig. 4). These results raise the possibility that although LIMK1 and cofilin are required for cell locomotion in general, SSH1L plays a more specific role; namely, in setting the direction of cell movement.

To further investigate this possibility, the chemotactic response of Jurkat cells in an SDF-1α gradient was analyzed using Dunn chambers (Zicha et al., 1991; Allen et al., 1998). Jurkat cells were transfected with siRNA plasmids, and their migration tracks in the bridge of a Dunn chemotaxis chamber were traced by using time-lapse video microscopy. Although control siRNA cells preferentially migrated up the SDF-1α gradient, the chemotactic responses of SSH1L, LIMK1, or cofilin siRNA cells were significantly suppressed (Fig. 5 A). Quantitative analyses revealed that LIMK1 or cofilin siRNA significantly decreased both the net translocation distance (straight distance from the start to the end point) and the migration speed (total length of the migration path per hour; Fig. 5, B and C). In contrast, the net translocation distance and migration speed of SSH1L siRNA cells were 35 and 69% of the values of control cells (Fig. 5, B and C). These data suggest that SSH1L siRNA cells retained their migration potential to appreciable levels but

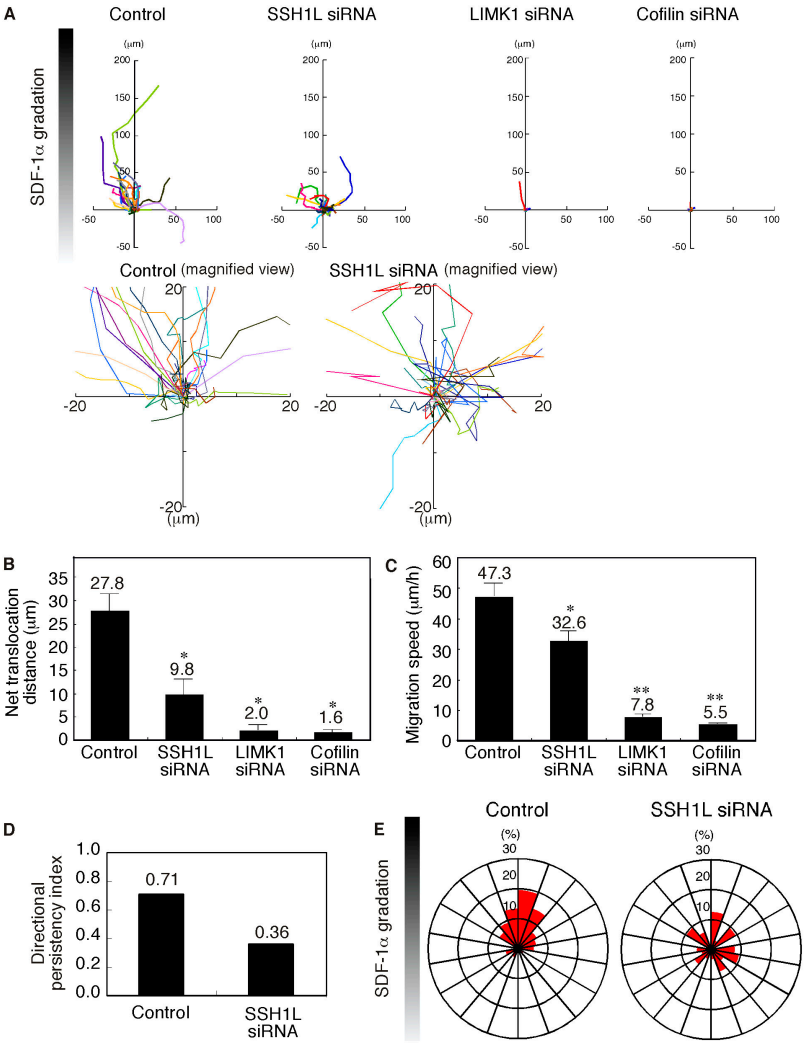

Figure 5. **Effect of SSH1L, LIMK1, or cofilin siRNA on SDF-1α–induced T cell chemotaxis in Dunn chambers.** Jurkat cells were transfected with siRNA plasmids for SSH1L, LIMK1, cofilin, or empty plasmid (control) and were analyzed for their ability to migrate in an SDF-1α gradient in the Dunn chamber during a 50-min period. (A) The migration paths of 30 randomly chosen cells were traced for 50 min. The intersection of the x and y axes was taken to be the starting point of each cell path, whereas the source of SDF-1α was at the top. Magnified views of the paths of control cells and SSH1L siRNA cells are also shown. (B) The net translocation distance (straight distance from the start to the end point) of each cell over the 50-min period is shown as the mean ± SEM (error bars) of the paths of 50 randomly chosen cells. *, $P < 0.01$ compared with control cells. (C) The migration speed (total length of the migration path per hour) of each cell is shown as the mean ± SEM of the paths of 50 randomly chosen cells. *, $P < 0.05$; **, $P < 0.01$ compared with control cells. (D) The directional persistency index (the ratio of the net translocation distance to the cumulative length of migration path) of control and SSH1L siRNA cells. (E) Circular histograms showing the percentage of cells whose final position was located within each of 18 equal sectors (20°). The source of SDF-1α was at the top. Data from control and SSH1L siRNA cells are shown.

turned more frequently than the control cells. Indeed, we found that SSH1L siRNA cells frequently changed direction compared with control cells (Fig. 5 A, magnified views). As a result, the index of the directional persistency (the ratio of the net translocation distance to the cumulative length of migration path) of SSH1L siRNA cells (0.36) was significantly lower than that of control cells (Fig. 5 D; 0.71). In addition, circular histograms showing the overall directionality of cell migration revealed that although 73% of control cells moved to positions within a 120° arc facing the SDF-1α source, only 33% of the SSH1L siRNA cells moved in this direction (Fig. 5 E), indicating that SSH1L siRNA cells migrated in random directions. Together, these findings suggest that LIMK1 and cofilin play an essential role in cell motility, whereas SSH1L is primarily involved in establishing or maintaining the directionality of cell movement.

Effects of LIMK1, SSH1L, or cofilin knockdown on SDF-1α–induced polarized lamellipodium formation

To elucidate the mechanisms by which SSH1L, LIMK1, or cofilin siRNA impaired T cell migration and chemotaxis, alterations in cell morphology and actin cytoskeleton were analyzed by time-lapse fluorescence analysis of live cells expressing YFP-actin (Fig. 6 A and Videos 4–7, available at http://www.jcb.org/cgi/content/full/jcb.200504029/DC1) and rhodamine-phalloidin staining of fixed cells (Fig. 6 B) before and after SDF-1α stimulation. Although control Jurkat cells exhibited a round and symmetrical morphology before SDF-1α stimulation, they generated multiple F-actin–rich membrane protrusions around the cell at 1 min after SDF-1α exposure, and these protrusions were then converted to a single lamellipodial protrusion on one side of the cell by 5 min (Fig. 6, A and B, control; and Video 4). This polarized cell morphology appears to support the directional migration of the cell. The total F-actin content per cell, which was measured by the fluorescence intensity of rhodamine-phalloidin, increased about twofold 10 min after SDF-1α stimulation (Fig. S1, available at http://www.jcb.org/cgi/content/full/jcb.200504029/DC1). In contrast, cofilin siRNA induced aberrant F-actin assembly and multiple large protrusions in the periphery of the cell both before and after SDF-1α stimulation (Fig. 6, A and B, cofilin siRNA; and Video 5). The total F-actin contents in cofilin siRNA cells before and after SDF-1α treatment were significantly higher than those in control cells (Fig. S1). The abnormal accumulation of F-actin suggests that cofilin controls actin filament dynamics by accelerating F-actin disassembly. The inappropriate F-actin assembly in cofilin siRNA cells was not affected by SDF-1α stimulation, suggesting that the cofilin knockdown cells failed to migrate as a result of their inability to rearrange the actin cytoskeleton in response to SDF-1α.

LIMK1 or SSH1L siRNA had no apparent effect on the overall cell shape and F-actin distribution in unstimulated cells. However, in contrast to control cells, LIMK1 siRNA cells formed only faint and immature membrane protrusions (Fig. 6, A and B, LIMK1 siRNA; and Video 6) and did not significantly increase the F-actin content (Fig. S1) after SDF-1α stimulation, which suggests that LIMK1 plays an essential role for SDF-1α–induced F-actin assembly and lamellipodium formation after cell

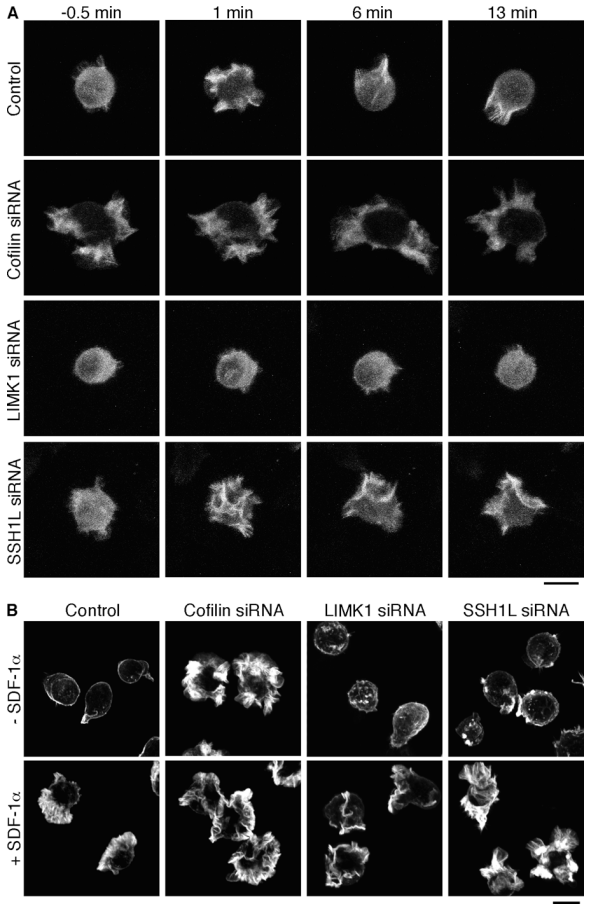

Figure 6. **Effect of cofilin, LIMK1, or SSH1L siRNA on F-actin assembly and membrane protrusion formation before and after SDF-1α stimulation.** (A) Time-lapse fluorescence analysis. Jurkat cells cotransfected with YFP-actin and siRNA plasmids for mutated SSH1L (control), cofilin, LIMK1, or SSH1L were analyzed by time-lapse fluorescence microscopy, making use of YFP fluorescence. Numbers indicate the times after SDF-1α stimulation. See Videos 4–7 (available at http://www.jcb.org/cgi/content/full/jcb.200504029/DC1). (B) Jurkat cells transfected with siRNA plasmids were left unstimulated (top) or stimulated for 5 min with SDF-1α (bottom) and were fixed and stained with rhodamine-phalloidin to visualize F-actin. Bars, 10 μm.

stimulation. Consistent with this, our previous study showed that the inhibition of LIMK1 activity by an inhibitory peptide suppressed SDF-1α–induced actin filament assembly and chemotaxis (Nishita et al., 2002). In SSH1L siRNA cells (in marked contrast to control cells), multiple protrusions that were produced in the initial stage of cell stimulation were not converted to the single lamellipodium even after 5–20 min of SDF-1α stimulation (Fig. 6, A and B, SSH1L siRNA; and Video 7), which may explain why SSH1L knockdown cells lost their directionality of migration in the chemotaxis assay. The inability of SSH1L siRNA cells to convert the initial multiple protrusions to the single lamellipodium suggests that SSH1L plays an essential role in limiting the membrane protrusion to one direction.

Trp-458 is critical for the F-actin–mediated activation of SSH1L

As SSH1L is highly activated by its association with F-actin (Nagata-Ohashi et al., 2004), we hypothesized that the F-actin–

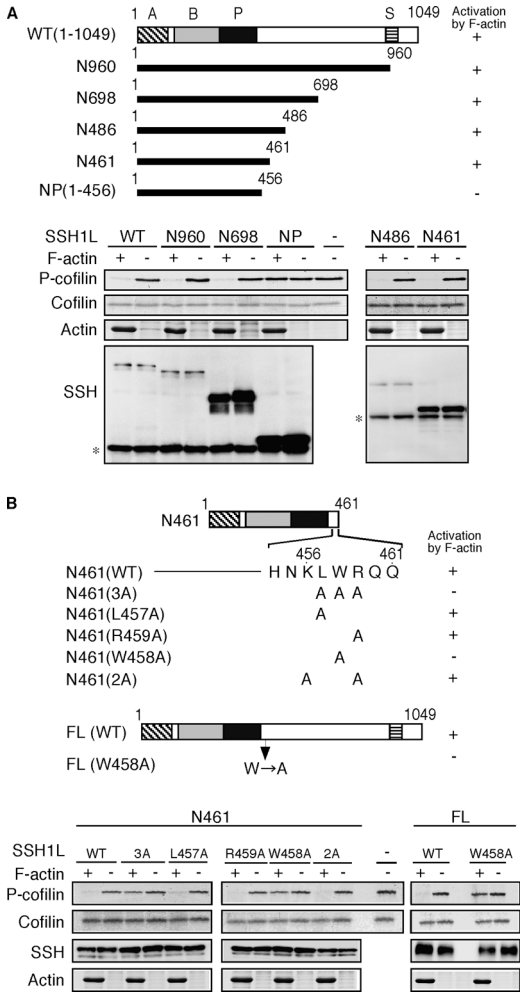

Figure 7. **Trp-458 is critical for the F-actin–mediated activation of SSH1L.** (A) The role of amino acids 457–461 in F-actin–mediated SSH1L activation. Schematic structures of SSH1L and deletion mutants are shown. The conserved regions in the SSH family are indicated by the A, B, P (phosphatase), and S (Ser-rich) domains. Wild-type (WT) and deletion mutants of (myc + His)-tagged SSH1L were expressed in 293T cells, immunoprecipitated with an anti-myc antibody, and subjected to in vitro phosphatase assays using cofilin-$(His)_6$ as a substrate in the presence or absence of F-actin. P-cofilin levels were measured by Pro-Q staining. Total cofilin and actin were measured by Coomassie blue staining. The expression of SSH1L mutants was analyzed by immunoblotting with the anti-myc antibody. *, Ig heavy chain. (B) Trp-458 is required for F-actin–mediated SSH1L activation. Point mutants of N461 and full-length (FL) SSH1L were subjected to in vitro cofilin phosphatase assays as described in A. Arrow indicates the replacement of Trp-458 with Ala.

mediated activation of SSH1L is critical for polarized cell migration. To identify the sites of SSH1L that are required for F-actin–mediated activation, a series of COOH-terminally deleted mutants of SSH1L were constructed. The truncated proteins were subjected to in vitro cofilin phosphatase assays in the absence or presence of F-actin by using P-cofilin as a substrate (Fig. 7 A). As previously reported (Nagata-Ohashi et al., 2004), wild-type (WT) SSH1L was activated by F-actin, but the COOH-terminally deleted mutant NP (composed of amino acid residues 1–456) was not. Unexpectedly, the other COOH-terminally deleted mutants (N960, N698, N486, and N461) were all activated by F-actin. This indicates that the region corresponding to amino acids 457–461 is required for the F-actin–mediated activation of SSH1L. To further define the residues that are essential for activation, various point mutants of N461 were constructed and subjected to cofilin phosphatase assays with or without F-actin (Fig. 7 B). The assays revealed that W458A (Trp-458 replaced by Ala) and 3A (Leu-457, Trp-458, and Arg-459 replaced by Ala) mutants of N461 were only weakly activated in the presence of F-actin, whereas other point mutants were remarkably activated by F-actin to a level similar to that of WT N461. Furthermore, the full-length SSH1L(W458A) mutant was poorly activated by F-actin (Fig. 7 B). Thus, Trp-458 is a critical residue for SSH1L activation by F-actin. Kinetic analysis revealed that although WT SSH1L was ~10-fold activated by F-actin, SSH1L(W458A) was only approximately twofold activated by F-actin (Fig. S2 A, available at http://www.jcb.org/cgi/content/full/jcb.200504029/DC1). However, SSH1L(W458A) retained the basal cofilin phosphatase activity (activity in the absence of F-actin) to a level similar to that of WT SSH1L (Fig. S2 B), which indicates that Trp-458 is specifically involved in the process of F-actin–mediated activation.

F-actin–mediated SSH1L activation is required for SDF-1α–induced polarized lamellipodium formation and chemotaxis in Jurkat cells

We next analyzed whether the expression of WT or mutated SSH1L could rescue the inhibitory effect of SSH1L siRNA on chemotaxis. We constructed an siRNA-resistant (sr) SSH1L cDNA bearing two nucleotide mutations in the siRNA target sequence that did not lead to amino acid substitution. Cotransfection of Jurkat cells with sr-SSH1L(WT) along with the SSH1L siRNA plasmid caused chemotactic activity toward SDF-1α in Transwell assays to recover considerably (Fig. 8 A). This indicates that the inhibitory effect of SSH1L siRNA on T cell chemotaxis is attributable to the specific knockdown of endogenous SSH1L expression. Notably, unlike sr-SSH1L(WT), cotransfection with either a phosphatase-dead sr-SSH1L(C393S), an F-actin–insensitive sr-SSH1L(W458A), or the COOH-terminally deleted NP(1–456) mutant (that has no siRNA target sequence and is not activated by F-actin) failed to rescue the chemotactic migration of SSH1L siRNA cells (Fig. 8 A). Phalloidin staining also revealed that SSH1L siRNA cells transfected with sr-SSH1L(WT) induced a relatively normal polarized cell morphology bearing a single lamellipodium, whereas cells that were transfected with sr-SSH1L(C393S), sr-SSH1L(W458A), or NP(1–456) exhibited phenotypes that were similar to those of SSH1L siRNA cells (Fig. 8 B and not depicted). Quantitative analyses showed that control and SSH1L siRNA cells preferentially exhibited cell morphologies that were categorized into class 2 (with a single lamellipodium) and 3 (with multiple lamellipodia around the cell), respectively, after SDF-1α stimulation (Fig. 8 C). The class 3 cell morphology reverted to class 2 morphology in SSH1L siRNA cells upon the expression of sr-SSH1L(WT) but not sr-SSH1L(C393S), sr-SSH1L(W458A), or NP(1–456) (Fig. 8 C). These findings suggest that both phosphatase activity and the

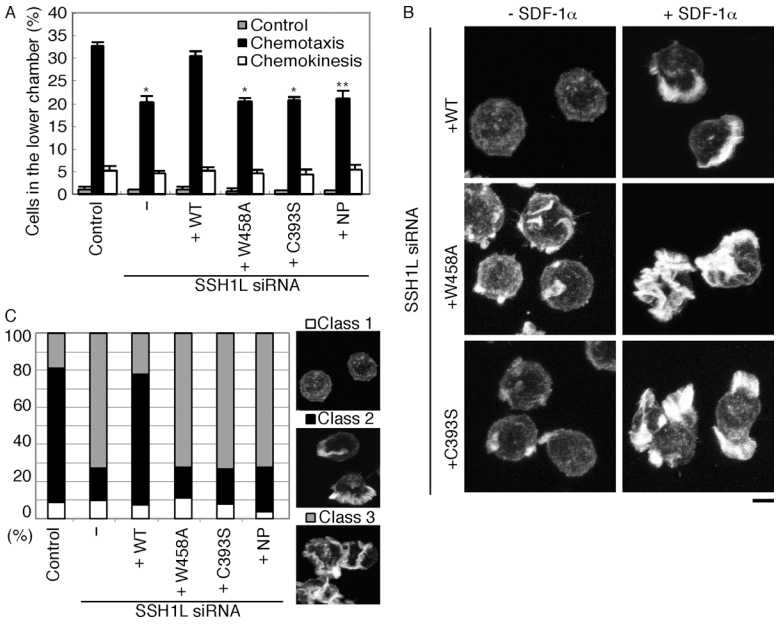

Figure 8. **F-actin–mediated activation of SSH1L is critical for polarized lamellipodium formation and chemotaxis.** (A) Expression of siRNA-resistant (sr) SSH1L(WT), but not sr-C393S, sr-W458A, or NP mutant, rescues the inhibitory effect of SSH1L siRNA on T cell chemotaxis. Jurkat cells were cotransfected with SSH1L siRNA plasmids together with expression plasmids for sr-SSH1L(WT), sr-C393S, sr-W458A, or NP mutants cultured for 60 h and were subjected to Transwell culture chamber assays as described in Fig. 4. *, $P < 0.005$; **, $P < 0.05$, compared with cells transfected with empty vector. Error bars represent SEM. (B) Expression of sr-SSH1L(WT), but not sr-C393S or sr-W458A mutant, recovers the SDF-1α–induced polarized F-actin assembly in SSH1L siRNA cells. Jurkat cells transfected as in A were cultured for 60 h, stimulated with 5 nM SDF-1α for 5 min, and stained with rhodamine-phalloidin for F-actin as described in Fig. 6 B. Bar, 5 μm. (C) Quantitative analysis of cell morphology changes. Jurkat cells transfected with SSH1L siRNA plasmids together with the indicated sr-SSH1L expression plasmids were cultured for 60 h, stimulated with 5 nM SDF-1α for 5 min, and stained as in B. Cells were categorized into three classes, as shown on the right: class 1 (round cells without a lamellipodium), class 2 (cells with a single lamellipodium), and class 3 (cells with multiple lamellipodia around the cells). The percentages of cells in each class are shown as the means of triplicate experiments (200–300 cells were counted in each experiment).

F-actin–mediated activation of SSH1L are required for the SDF-1α–induced polarized cell shape formation and chemotactic response of Jurkat cells.

We also examined whether the expression of chick sr-LIMK1 or reaction product mimic S3E-cofilin (Ser-3 is replaced by Glu) could rescue the phenotypes of LIMK1 siRNA cells. However, the expression of chick LIMK1 or S3E-cofilin did not significantly rescue the inhibitory effects of LIMK1 siRNA on chemotactic and chemokinetic responses (Fig. S3 A, available at http://www.jcb.org/cgi/content/full/jcb.200504029/DC1). The expression of chick LIMK1 in LIMK1 siRNA cells induced aberrant F-actin assembly and multiple protrusions around the cell after SDF-1α stimulation (Fig. S3 B), which indicates that chick LIMK1 phosphorylates endogenous cofilin and, thereby, inactivates the actin filament–disassembling activity of cofilin. The expression of S3E-cofilin had no apparent effect on the morphology and actin assembly of LIMK1 siRNA cells (Fig. S3 B) probably because S3E-cofilin has neither actin-binding activity nor the ability to affect the activity of endogenous cofilin.

Discussion

Based on our observations, we propose the following model of LIMK1 and SSH1L actions in SDF-1α–induced actin filament remodeling and chemotactic migration of Jurkat cells (Fig. 9). In the initial stage of cell stimulation, SDF-1α induces the activation of LIMK1 through Rac activation (Nishita et al., 2002), and this transiently increases P-cofilin levels for up to 5 min and induces F-actin assembly; multiple membrane protrusions are first generated around the cell periphery at ~1 min and are transformed to the single lamellipodium by 5 min. Because LIMK1 siRNA significantly suppressed SDF-1α–induced cofilin phosphorylation and lamellipodial protrusion formation, LIMK1 seems to play a critical role in lamellipodium formation during the initial stage of cell stimulation by inactivating cofilin and shifting the balance of actin filament dynamics to actin filament polymerization and stabilization. Because the extension of the lamellipodium provides the driving force for cell migration, impaired lamellipodium formation is a likely reason for the failure of LIMK1 knockdown cells to migrate in response to SDF-1α.

SSH1L accumulates in the lamellipodium by 1 min after SDF-1α stimulation. As SSH1L is activated by associating with F-actin, it probably becomes active immediately after the lamellipodia have formed and SSH1L has subsequently translocated

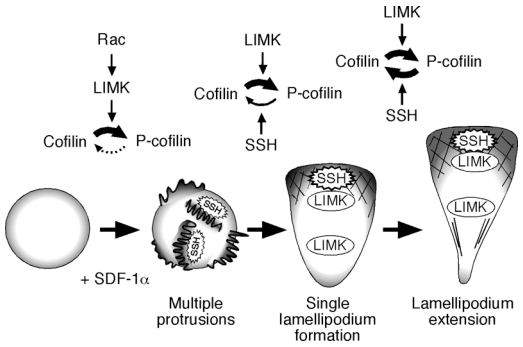

Figure 9. **A model for the LIMK1- and SSH1L-mediated spatiotemporal regulation of cofilin activity during SDF-1α–induced polarized F-actin assembly and cell migration.** The unstimulated Jurkat cell has a round, symmetrical shape. Exposure of the cell to SDF-1α induces the activation of LIMK1 through Rac and leads to a transient increase in P-cofilin levels, which is required for the formation of F-actin–rich lamellipodial protrusions in the initial stages of cell response. SSH1L translocates to the lamellipodia and is activated by associating with F-actin. Because SSH1L knockdown cells retain multiple protrusions during the cell stimulation, SSH1L is required for the conversion of multiple protrusions to the single lamellipodium. In later stages, SSH1L locally stimulates cofilin activation and actin filament turnover in the lamellipodium in the front of the cell, whereas LIMK1 is diffusely distributed in the cell and may help to stabilize actin filaments in the rear of the cell.

to this region. In unstimulated cells, SSH1L may be sequestered in the cytoplasm and protected from F-actin–mediated activation by associating with 14-3-3 proteins (Nagata-Ohashi et al., 2004). The accumulation of cofilin, but not P-cofilin, in the lamellipodia suggests that SSH1L locally activates cofilin in the lamellipodia. Thus, we propose that once actin filaments assemble in response to SDF-1α, they trigger the local activation of SSH1L and cofilin and, thereby, stimulate their own dynamics so that the dynamic nature of the lamellipodium is ensured.

The mechanism that induces the conversion of multiple protrusions to the single lamellipodium to form polarized F-actin assembly during 1–5 min after cell stimulation is not well understood. It is also not known whether the formation of multiple protrusions is the generally occurring event in the first stage of cell stimulation regardless of the conditions of uniform or gradient concentrations of SDF-1α. SSH1L siRNA cells, in marked contrast to control cells, retained multiple protrusions for up to 20 min after SDF-1α stimulation, which strongly suggests that SSH1L is required for the formation of the single lamellipodium and polarized cell morphology. In SSH1L knockdown cells, only LIMK1 is activated after SDF-1α stimulation, and, as a result, cofilin-phosphorylating activity dominates cofilin phosphatase activity throughout the cell. This leads to the less dynamic nature of the lamellipodia and the failure of actin filament remodeling and holds on multiple membrane protrusions around the cell. This probably causes the loss of directionality in the migration of SSH1L siRNA cells. Consistent with this observation, the overexpression of LIMK1 induced multiple protrusions in random directions and impaired the formation of polarized morphology and directional migration of fibroblasts (Dawe et al., 2003).

On the other hand, phosphatidylinositol-3 kinase (PI3K) and its lipid products are known to be essential for the formation of polarized membrane protrusion in the chemotactic responses of neutrophils and *Dictyostelium discoideum* cells (Rickert et al., 2000; Merlot and Firtel, 2003; Van Haastert and Devreotes, 2004). Once one of the protrusions is selected stochastically or dependently on the SDF-1α gradient, the amplification mechanism by a positive feedback loop between PI3K, Rac, and F-actin (Wang et al., 2002; Weiner et al., 2002) may induce polarized lamellipodium formation in one direction. As LIMK1 siRNA cells continuously exhibit faint and multiple protrusions for 1–20 min after cell stimulation, LIMK1 (as one of the effectors of Rac) may also play a role in the conversion of multiple protrusions to a single lamellipodium. Thus, both excessive (as seen in SSH1L siRNA cells) and insufficient cofilin phosphorylation (as seen in LIMK1 siRNA cells) result in the sustained formation of multiple protrusions in random directions and the loss of cell polarity, although the protrusions are significantly weak in the latter case. It is likely that the precise control of cofilin phosphorylation and dephosphorylation activities is required for polarized F-actin assembly. In addition, the inability of the W458A or NP mutant of SSH1L to rescue the phenotypes of SSH1L siRNA cells suggests that SSH1L translocation to the lamellipodium and its activation by F-actin are essential to the construction of polarized cell morphology and directional cell migration.

In the later stages of the cell response (after polarity is formed), both LIMK1 and SSH1L are activated. As LIMK1 is diffusely distributed in the cytoplasm and SSH1L is recruited to the lamellipodium, it appears that both LIMK1 and SSH1L are active in the front, but only LIMK1 is active in the rear of the cell (Fig. 9). This spatially distinct distribution of LIMK1 and SSH1L could restrict cofilin activity to the front of migrating cells, and the local activation of cofilin in the front can stimulate actin filament turnover for lamellipodium extension. Previous studies have shown that the temporal and spatial regulation of PI3K activity and its antagonistic lipid phosphatase PTEN generates the polarized accumulation of $PI(3,4,5)P_3$ in the anterior region of migrating cells (Funamoto et al., 2002; Iijima and Devreotes, 2002), and a local excitation–global inhibition model was proposed to explain the polarity formation and maintenance in the chemotactic response (Devreotes and Janetopoulos, 2003). A similar mechanism, which consisted of the local excitation of cofilin by F-actin–associated SSH1L and its global inhibition by diffusely distributed LIMK1, might be responsible for the local activation of cofilin in the leading edge of the cell. The activation of both LIMK1 and SSH1L in the lamellipodium could cooperatively accelerate the recycling of cofilin and actin via the LIMK1-stimulated dissociation of cofilin–actin complexes that are released from the pointed ends of actin filaments (Rosenblatt and Mitchison, 1998). Alternatively, SSH1L might down-regulate LIMK1 activity by dephosphorylation, as reported by Soosairajah et al. (2005), and, thereby, further enhance the cofilin dephosphorylation/activation in the front of the cell.

Although both cofilin and SSH1L siRNA cells protrude multiple lamellipodia, cofilin siRNA cells almost completely lose cell migration activity, whereas SSH1L siRNA cells are competent for cell migration but only lose directionality. Why do these cells exhibit such distinct phenotypes in migration? In time-lapse analyses in Fig. 6 A and Videos 5 and 7, cofilin siRNA appears to depress the motility of lamellipodia, whereas SSH1L siRNA cells retain the dynamic nature of protrusions. Thus, it is likely that actin filament dynamics differ between cofilin and SSH1L knockdown cells. In contrast to cofilin siRNA cells, where cofilin expression is directly suppressed, SSH1L siRNA cells may retain some populations of cofilin in active state by global dephosphorylation of P-cofilin by other cofilin phosphatases such as SSH2, SSH3, or chronophin (Niwa et al., 2002; Gohla et al., 2005).

Recent studies on EGF-stimulated carcinoma cells suggested that cofilin may have a role in initiating the actin filament polymerization by severing actin filaments and exposing free barbed ends for polymerization (Ghosh et al., 2004). This could occur under conditions in which polymerization-ready actin monomers are abundant (DesMarais et al., 2005). However, in most cases, the mutation or knockdown of cofilin expression in yeast, *Drosophila melanogaster,* and mammalian cells resulted in excessive F-actin assembly (Gunsalus et al., 1995; Lappalainen and Drubin, 1997; Chen et al., 2001; Rogers et al., 2003; Hotulainen et al., 2005), which indicates that at least in the steady state of these cells, cofilin regulates actin filament dynamics by accelerating actin filament disassembly.

Consistent with these observations, we showed in this study that cofilin siRNA induced abnormal F-actin accumulation in Jurkat cells before and after SDF-1α stimulation; LIMK1 siRNA suppressed lamellipodium formation, and SSH1L siRNA induced aberrant F-actin assembly after SDF-1α stimulation. These results suggest that in Jurkat cells, cofilin regulates actin turnover by stimulating actin filament disassembly, and LIMK1 and SSH1L regulate actin filament dynamics through inactivating and activating cofilin, respectively.

In summary, our data indicate that phosphoregulation of cofilin activity by LIMK1 and SSH1L is essential for SDF-1α–induced T cell migration and chemotaxis. LIMK1 regulates cell movement by producing a stimulus-dependent membrane protrusion, and the subsequent activation of SSH1L in the lamellipodium controls the directionality of cell migration by stimulating cofilin in this region. This LIMK1- and SSH1L-mediated spatial and temporal regulation of cofilin activity appears to be important for establishing and maintaining a polarized cell morphology and chemotactic response. As SDF-1α is a potent chemotactic factor for various cells (Zlotnik and Yoshie, 2000; Muller et al., 2001; Zhu et al., 2002; Arakawa et al., 2003), future studies will shed light on the roles of cofilin phosphoregulation in various pathophysiologically important processes, including immune responses, neuronal development, and tumor metastasis.

Materials and methods

Materials

SDF-1α and rhodamine-phalloidin were purchased from PeproTech and Invitrogen, respectively. The mouse mAb to β-actin was purchased from Sigma-Aldrich. Rabbit pAbs to LIMK1, P-cofilin, cofilin, and SSH1L were generated as described previously (Okano et al., 1995; Toshima et al., 2001; Kaji et al., 2003). The rhodamine-conjugated anti–mouse IgG antibody and the FITC-conjugated anti–rabbit IgG antibody were purchased from Chemicon.

Plasmid construction

Plasmids encoding YFP- or CFP-tagged LIMK1, SSH1L, and actin were constructed as described previously (Endo et al., 2003; Nishita et al., 2004). Plasmids for phosphatase-dead SSH1L(C393S), NP(N456), S3E-cofilin, and chick LIMK1 were constructed as described previously (Niwa et al., 2002; Endo et al., 2003; Nagata-Ohashi et al., 2004). The expression plasmid for COOH-terminally (myc + His) tagged human SSH1L was constructed by using the pcDNA3.1/myc-His(+) vector (Invitrogen). The plasmids encoding COOH-terminally deleted and/or point-mutated (myc + His) SSH1L proteins were generated by PCR amplification and subcloned into the pcDNA3.1/myc-His(+) vector. Oligonucleotides were annealed and subcloned into pSUPER vector plasmids (provided by R. Agami, Netherlands Cancer Institute, Amsterdam, Netherlands) as described previously (Brummelkamp et al., 2002) to generate siRNA plasmids against human LIMK1, SSH1L, cofilin, and GFP. Oligonucleotides were composed of pairs of the following 19-base target sequences plus a nine-base spacer: LIMK1 (nucleotide positions from the start ATG codon, 209–237; GAAGGACTACTGGGCCCGC), SSH1L (nucleotide positions 2,329–2,347; TCGTCACCCAAGAAAGATA), cofilin (nucleotide positions 288–306; GGAGGATCTGGTGTTTATC), and GFP (GCAGCACGACTTCTTCAAG). To construct expression plasmids encoding the sr-SSH1L (WT, C393S, or W458A) protein, two bases in the 19-base target sequence in the corresponding (myc + His)-SSH1L cDNA were mutated (TCTTCCCCCAAGAAAGATA) by PCR amplification and subcloning.

Cell culture and transfection

Jurkat human leukemic T cells were obtained from T. Kudo (Cell Resource Center for Biomedical Research, Tohoku University, Sendai, Japan) and were maintained in Roswell Park Memorial Institute (RPMI) 1640 medium supplemented with 9% FCS. For transfection, $\sim 10^7$ cells were mixed with plasmids in 400 μl of electroporation medium (RPMI 1640 medium containing 20% FCS and 25 mM Hepes, pH 7.4) and were electroporated at 280 V and 975 μF using a Gene Pulser II (Bio-Rad Laboratories). After electroporation, the cells were cultured for 18–60 h in RPMI 1640 medium supplemented with 10% FCS. The transfection efficiency was >90%, as assessed by the transfection of YFP cDNA plasmids.

Immunoprecipitation and immunoblotting

Whole Jurkat cell lysates were prepared as described previously (Nishita et al., 2002). After centrifugation, the lysates were subjected to SDS-PAGE and immunoblotted with antibodies against P-cofilin or cofilin as described previously (Toshima et al., 2001). To analyze endogenous LIMK1 or SSH1L, the cell lysates were immunoprecipitated and immunoblotted with anti-LIMK1 or anti-SSH1L antibodies.

Cell staining

Jurkat cells that were suspended in RPMI 1640 medium containing 25 mM Hepes, pH 7.4, and 0.2% BSA were incubated for 20 min at 37°C. The cells were then plated on coverslips and allowed to attach for 5 min at 37°C. The attached cells were stimulated with 5 nM SDF-1α for 0–20 min, fixed with 4% PFA for 20 min and cold 100% methanol for 10 min at −20°C, blocked with 2% FCS for 30 min, and costained with anticofilin or anti–P-cofilin rabbit pAbs and anti–β-actin mouse mAb. The FITC-conjugated anti–rabbit and rhodamine-conjugated anti–mouse IgG antibodies were used as second antibodies. To stain F-actin by rhodamine-phalloidin, the methanol fixation step was omitted. Stacked optical sections were obtained and merged by using a laser scanning confocal imaging system (LSM 510; Carl Zeiss MicroImaging, Inc.) equipped with a plan Apo NA 1.4 63× oil immersion objective lens (Carl Zeiss MicroImaging, Inc.).

Time-lapse fluorescence analysis

For time-lapse imaging, Jurkat cells were transfected with plasmids for YFP- and/or CFP-fused protein. Images of stacked optical sections were collected every 30 s for up to 10–20 min after SDF-1α stimulation by using the aforementioned laser scanning confocal microscope and objective lens.

Cell migration assays

For the cell migration assays using Transwell culture chambers (5-μm pore size; Costar), the lower wells were filled with 600 μl of medium (RPMI 1640 containing 0.5% BSA and 25 mM Hepes, pH 7.4) with or without 5 nM SDF-1α. Jurkat cells (2×10^5 cells) suspended in 100 μl of medium were loaded into the upper wells. 5 nM SDF-1α was added only to the lower well (for chemotaxis assays), to both the lower and upper wells (for chemokinesis assays), or to neither well (control). After incubation for 3 h at 37°C, the cells that had migrated into the lower wells were counted and shown as percentages of the input cells. Chemotaxis was also assessed by directly observing the migrating cells in an SDF-1α gradient using the Dunn chamber (Weber Scientific International; Allen et al., 1998). In these assays, Jurkat cells that were suspended in RPMI 1640 medium containing 9% FBS were loaded into both the inner and outer wells of the chamber, and the wells were covered with a coverslip. The medium in the outer well was replaced with the same medium containing 5 nM SDF-1α. After incubation for 3 h at 37°C, cells migrating on the bridge between the inner and outer wells were observed by using an inverted microscope (DMIRBE; Leica). Time-lapse images were digitally captured every 30 s for 50 min with a cooled CCD camera (CoolSNAP HQ; Roper Scientific). To track migration paths, a series of images were analyzed using IPLab image analysis software (Scanalytics), and the data were plotted with Microsoft Excel. Net translocation distance was determined as the straight distance between the start and the end points during a 50-min period. Migration speed was calculated from the total length of the migration path during a 50-min period. To visualize the directionality of cell migration, we constructed circular histograms showing the percentage of cells whose final position relative to a common origin was within one of 18 20° sectors.

In vitro cofilin phosphatase assay

(Myc + His)-tagged SSH1L and its mutants expressed in 293T cells were immunoprecipitated with anti-myc antibody and were incubated with 100 ng cofilin-$(His)_6$ for 1 h at 30°C in 20 μl lysis buffer in the absence or presence of 5 μg F-actin as described previously (Nagata-Ohashi et al., 2004). The reaction mixtures were then subjected to SDS-PAGE. P-cofilin was analyzed by staining with the Pro-Q Diamond phosphoprotein gel stain kit (Invitrogen), whereas cofilin and actin were analyzed by Coomassie brilliant blue staining. SSH1L and its mutants were analyzed by immunoblotting with an anti-myc antibody.

Online supplemental material

Fig. S1 shows changes in the total F-actin content in Jurkat cells before and after SDF-1α stimulation. Fig. S2 shows the kinetic analyses of cofilin phosphatase activity of WT, W458A, and C393S mutants of SSH1L with or without F-actin. Fig. S3 shows the effects of chick LIMK1 or S3E-cofilin expression on the phenotypes of LIMK1 siRNA cells. Video 1 is the three-dimensional projection of the cell that was stimulated for 5 min with SDF-1α in Fig. 2 A. Video 2 shows the time-lapse fluorescence of Jurkat cell coexpressing CFP-LIMK1 and YFP-SSH1L. Video 3 shows the time-lapse fluorescence of a Jurkat cell coexpressing YFP-actin and CFP-SSH1L. Videos 4–7 are the time-lapse fluorescence videos of YFP-actin–expressing control and various knockdown Jurkat cells (corresponds to Fig. 6 A), which are listed as follows: Video 4, control cell; Video 5, cofilin siRNA cell; Video 6, LIMK1 siRNA cell; and Video 7, SSH1L siRNA cell. Online supplemental material is available at http://www.jcb.org/cgi/content/full/jcb.200504029/DC1.

We thank Dr. R. Agami for the pSUPER plasmid and Dr. K. Nagata-Ohashi, Dr. R. Niwa, Dr. T Uemura, Dr. Y. Minami, and M. Ohara for helpful comments and encouragement.

This work was supported by a grant-in-aid for Creative Scientific Research and by the 21st Century Centers of Excellence Program from the Ministry of Education, Culture, Sports, Science, and Technology of Japan.

Submitted: 6 April 2005
Accepted: 20 September 2005

References

Allen, W.E., D. Zicha, A.J. Ridley, and G.E. Jones. 1998. A role for Cdc42 in macrophage chemotaxis. *J. Cell Biol.* 141:1147–1157.

Arakawa, Y., H. Bito, T. Furuyashiki, T. Tsuji, S. Takemoto-Kimura, K. Kimura, K. Nozaki, N. Hashimoto, and S. Narumiya. 2003. Control of axon elongation via an SDF-1α/Rho/mDia pathway in cultured cerebellar granule neurons. *J. Cell Biol.* 161:381–391.

Arber, S., F.A. Barbayannis, H. Hanser, C. Schneider, C.A. Stanyon, O. Bernard, and P. Caroni. 1998. Regulation of actin dynamics through phosphorylation of cofilin by LIM-kinase. *Nature.* 393:805–809.

Bailly, M., and G.E. Jones. 2003. Polarised migration: cofilin holds the front. *Curr. Biol.* 13:R128–R130.

Bamburg, J.R. 1999. Proteins of the ADF/cofilin family: essential regulators of actin dynamics. *Annu. Rev. Cell Dev. Biol.* 15:185–230.

Bamburg, J.R., and O.P. Wiggan. 2002. ADF/cofilin and actin dynamics in disease. *Trends Cell Biol.* 12:598–605.

Brummelkamp, T.R., R. Bernards, and R. Agami. 2002. A system for stable expression of short interfering RNAs in mammalian cells. *Science.* 296:550–553.

Chen, J., D. Godt, K. Gunsalus, I. Kiss, M. Goldberg, and F.A. Laski. 2001. Cofilin/ADF is required for cell motility during *Drosophila* ovary development and oogenesis. *Nat. Cell Biol.* 3:204–209.

Cramer, L.P. 1999. Roles of actin-filament disassembly in lamellipodium protrusion in motile cells revealed using the drug jasplakinolide. *Curr. Biol.* 9:1095–1105.

Dawe, H.R., L.S. Minamide, J.R. Bamburg, and L.P. CrAm. 2003. ADF/cofilin controls cell polarity during fibroblast migration. *Curr. Biol.* 13:252-257.

DesMarais, V., M. Ghosh, R. Eddy, and J. Condeelis. 2005. Cofilin takes the lead. *J. Cell Sci.* 118:19–26.

Devreotes, P., and C. Janetopoulos. 2003. Eukaryotic chemotaxis: distinctions between directional sensing and polarization. *J. Biol. Chem.* 278: 20445–20448.

Endo, M., K. Ohashi, Y. Sasaki, Y. Goshima, R. Niwa, T. Uemura, and K. Mizuno. 2003. Control of growth cone motility and morphology by LIM kinase and Slingshot via phosphorylation and dephosphorylation of cofilin. *J. Neurosci.* 23:2527–2537.

Franz, C.M., G.E. Jones, and A.J. Ridley. 2002. Cell migration in development and disease. *Dev. Cell.* 2:153–158.

Funamoto, S., R. Meili, S. Lee, L. Parry, and R.A. Firtel. 2002. Spatial and temporal regulation of 3-phosphoinositides by PI 3-kinase and PTEN mediates chemotaxis. *Cell.* 109:611–623.

Ghosh, M., X. Song, G. Mouneimne, M. Sidani, D.S. Lawrence, and J.S. Condeelis. 2004. Cofilin promotes actin polymerization and defines the direction of cell motility. *Science.* 304:743–746.

Gohla, A., J. Birkenfeld, and G.M. Bokoch. 2005. Chronophin, a novel HAD-type serine protein phosphatase, regulates cofilin-dependent actin dynamics. *Nat. Cell Biol.* 7:21–29.

Gunsalus, K., S. Bonaccorsi, E. Williams, F. Verni, M. Gatti, and M.L. Goldberg. 1995. Mutations in twinstar, a *Drosophila* gene encoding a cofilin/ADF homologue, result in defects in centrosome migration and cytokinesis. *J. Cell Biol.* 131:1243–1259.

Hotulainen, P., E. Paunolla, M.K. Vartiainen, and P. Lappalainen. 2005. Actin-depolymerizing factor and cofilin-1 play overlapping roles in promoting rapid F-actin depolymerization in mammalian nonmuscle cells. *Mol. Biol. Cell.* 16:649–664.

Iijima, M., and P. Devreotes. 2002. Tumor suppressor PTEN mediates sensing of chemoattractant gradients. *Cell.* 109:599–610.

Kaji, N., K. Ohashi, M. Shuin, R. Niwa, T. Uemura, and K. Mizuno. 2003. Cell cycle-associated changes in Slingshot phosphatase activity and roles in cytokinesis in animal cells. *J. Biol. Chem.* 278:33450–33455.

Lappalainen, P., and D.G. Drubin. 1997. Cofilin promotes rapid actin filament turnover in vivo. *Nature.* 388:78–82.

Merlot, S., and R.A. Firtel. 2003. Leading the way: directional sensing through phosphatidylinositol 3-kinase and other signaling pathways. *J. Cell Sci.* 116:3471–3478.

Moon, A., and D.G. Drubin. 1995. The ADF/cofilin proteins: stimulus-responsive modulators of actin dynamics. *Mol. Biol. Cell.* 6:1423–1431.

Muller, A., B. Homey, H. Soto, N. Ge, D. Catron, M.E. Buchanan, T. McClanahan, E. Murphy, W. Yuan, S.N. Wagner, et al. 2001. Involvement of chemokine receptors in breast cancer metastasis. *Nature.* 410:50–56.

Nagata-Ohashi, K., Y. Ohta, K. Goto, S. Chiba, R. Mori, M. Nishita, K. Ohashi, K. Kousaka, A. Iwamatsu, R. Niwa, et al. 2004. A pathway of neuregulin-induced activation of cofilin-phosphatase Slingshot and cofilin in lamellipodia. *J. Cell Biol.* 165:465–471.

Nishita, M., H. Aizawa, and K. Mizuno. 2002. Stromal cell-derived factor 1α activates LIM kinase 1 and induces cofilin phosphorylation for T-cell chemotaxis. *Mol. Cell. Biol.* 22:774–783.

Nishita, M., Y. Wang, C. Tomizawa, A. Suzuki, R. Niwa, T. Uemura, and K. Mizuno. 2004. Phosphoinositide 3-kinase-mediated activation of cofilin phosphatase Slingshot and its role for insulin-induced membrane protrusion. *J. Biol. Chem.* 279:7193–7198.

Niwa, R., K. Nagata-Ohashi, M. Takeichi, K. Mizuno, and T. Uemura. 2002. Control of actin reorganization by Slingshot, a family of phosphatases that dephosphorylate ADF/cofilin. *Cell.* 108:233–246.

Ohta, Y., K. Kousaka, K. Nagata-Ohashi, K. Ohashi, A. Muramoto, Y. Shima, R. Niwa, T. Uemura, and K. Mizuno. 2003. Differential activities, subcellular distribution and tissue expression patterns of three members of Slingshot family phosphatases that dephosphorylate cofilin. *Genes Cells.* 8:811–824.

Okano, I., J. Hiraoka, H. Otera, K. Nunoue, K. Ohashi, S. Iwashita, M. Hirai, and K. Mizuno. 1995. Identification and characterization of a novel family of serine/threonine kinases containing two N-terminal LIM motifs. *J. Biol. Chem.* 270:31321–31330.

Pantaloni, D., C. Le Clainche, and M.-F. Carlier. 2001. Mechanism of actin-based motility. *Science.* 292:1502–1506.

Pollard, T.D., and G.G. Borisy. 2003. Cellular motility driven by assembly and disassembly of actin filaments. *Cell.* 112:453–465.

Rickert, P., O.D. Weiner, F. Wang, H.R. Bourne, and G. Servant. 2000. Leukocytes navigate by compass: roles of PI3Kγ and its lipid products. *Trends Cell Biol.* 10:466–473.

Ridley, A.J., M.A. Schwartz, K. Burridge, R.A. Firtel, M.H. Ginsberg, G. Borisy, J.T. Parsons, and A.R. Horwitz. 2003. Cell migration: integrating signals from front to back. *Science.* 302:1704–1709.

Rogers, S.L., U. Wiedemann, N. Stuurman, and R.D. Vale. 2003. Molecular requirements for actin-based lamella formation in *Drosophila* S2 cells. *J. Cell Biol.* 162:1079–1088.

Rosenblatt, J., and T.J. Mitchison. 1998. Actin, cofilin and cognition. *Nature.* 393:739–740.

Soosairajah, J., S. Maiti, O. Wiggan, P. Sarmiere, N. Moussi, B. Sarcevic, R. Sampath, J.R. Bamburg, and O. Bernard. 2005. Interplay between components of a novel LIM kinase-slingshot phosphatase complex regulates cofilin. *EMBO J.* 24:473–486.

Theriot, J.A. 1997. Accelerating on a treadmill: ADF/cofilin promotes rapid filament turnover in the dynamic cytoskeleton. *J. Cell Biol.* 136:1165–1168.

Toshima, J., J.Y. Toshima, T. Amano, N. Yang, S. Narumiya, and K. Mizuno. 2001. Cofilin phosphorylation by testicular protein kinase 1 and its role in integrin-mediated actin reorganization and focal adhesion formation. *Mol. Biol. Cell.* 12:1131–1145.

Van Haastert, P.J., and P.N. Devreotes. 2004. Chemotaxis: signaling the way forward. *Nat. Rev. Mol. Cell Biol.* 5:626–634.

Wang, F., P. Herzmark, O. Weiner, S. Srinivasan, G. Servant, and H. Bourne. 2002. Lipid products of PI(3)Ks maintain persistent cell polarity and directional motility in neutrophils. *Nat. Cell Biol.* 4:513–518.

Weiner, O.D., P.O. Neilsen, G.D. Prestwich, M.W. Kirschner, L.C. Cantley, and H.R. Bourne. 2002. A PtdInsP_3- and Rho GTPase-mediated positive feedback loop regulates neutrophil polarity. *Nat. Cell Biol.* 4:509–512.

Welch, M.D., A. Mallavarapu, J. Rosenblatt, and T.J. Mitchison. 1997. Actin dynamics in vivo. *Curr. Opin. Cell Biol.* 9:54–61.

Yang, N., O. Higuchi, K. Ohashi, K. Nagata, A. Wada, K. Kangawa, E. Nishida, and K. Mizuno. 1998. Cofilin phosphorylation by LIM-kinase 1 and its role in Rac-mediated actin reorganization. *Nature.* 393:809–812.

Zlotnik, A., and O. Yoshie. 2000. Chemokines: a new classification system and their role in immunity. *Immunity.* 12:121–127.

Zhu, Y., T. Yu, X.C. Zhang, T. Nagasawa, J.Y. Wu, and Y. Rao. 2002. Role of the chemokine SDF-1 as the meningeal attractant for embryonic cerebellar neurons. *Nat. Neurosci.* 5:719–720.

Zicha, D., G.A. Dunn, and A.F. Brown. 1991. A new direct-viewing chemotaxis chamber. *J. Cell Sci.* 99:769–775.